IEEE Transactions on Nuclear Science, Vol. NS-32, No. 5, October 1985

REFINEMENT PROCEDURES OF BEAM POSITION MEASUREMENT IN THE TRISTAN ACCUMULATION RING

M. Tejima, H. Ishii, T. Shintake, J. Kishiro,
A. Ogata, T. Ieiri and Y. Mizumachi

National Laboratory for High Energy Physics (KEK)
Oho-machi, Tsukuba-gun, Ibaraki-ken, 305 JAPAN

Summary

High precision of about 0.1 mm is required in the beam position measurement of TRISTAN MR(main ring) which is now under construction. In this respect, position measurement in the TRISTAN AR(accumulation ring) is reviewed. We found that the statistical study of the accumulated measurement data gives very useful information on the performance of the monitor system. For example, repeated COD measurements during a beam storage showed not only reproducibility of the position measurement (0.05 mm) in the beam intensity range of factor 50 but also pointed out troubles caused by poor contact in coaxial switches. Moreover, it suggested the criterion to abandon erroneous data. Programs for such check has been prepared and has improved the efficiency of COD correction. Improvements have also been made in the calibration and in the mechanical setting of the monitor chambers.

Introduction

The operation of TRISTAN accumulation ring (AR) started at KEK from November 1983 (1) and the beam position monitor system has worked with good performance. During these two years, we have accumulated experiences which are useful for the design and the construction of the TRISTAN main ring (MR).

Position monitors in AR (2,3)

We have 83 monitor pickups for orbit measurement in AR, each one sitting at the side of a Q-magnet. A position electronics system is set in each of four local control buildings on the AR ring. Each one covers one fourth of monitors (20-22). A monitor chamber is just a part of an aluminum beam duct where four pickup electrodes are welded on to the wall as shown in Fig 1. (4) We use super-heterodyne detection scheme and pick up a harmonics of beam revolution.

Mapping calibration

We set the signal source at (X,Y) in a monitor chamber and measure the output voltages A,B,C,D, and then get the normalizations, Nx=(A+C-B-D)/(A+B+C+D) and Ny=(A+B-C-D)/(A+B+C+D). In this way, we get the relation between signal coordinates (Nx,Ny) and space coordinates (X,Y) for each monitor. We can practically

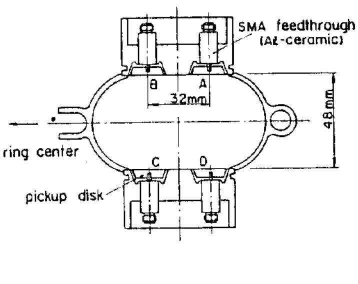

Fig 1 Position monitor chamber in the bending section

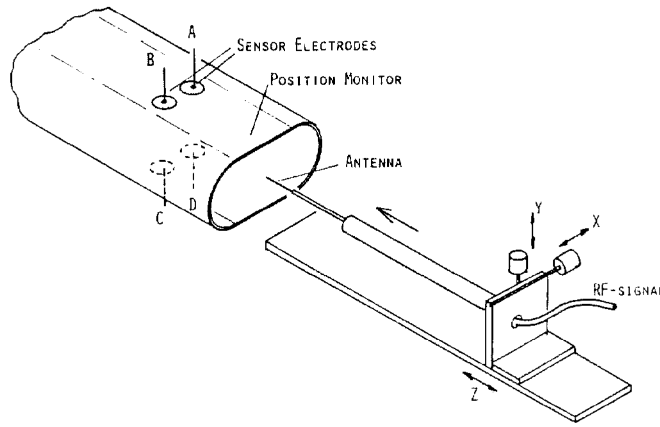

Fig 2 Setup for mapping calibration

represent it by the following third order polynominals,

$$X= \Sigma\, Px(i,j)*Nx^{i}*Ny^{j} \quad , \quad Y= \Sigma\, Py(i,j)*Nx^{i}*Ny^{j} \qquad (1)$$

with $0 \le i,j \le 3$, $0 \le i+j \le 3$. In these expressions, Px(0,0) and Py(0,0) gives the deviation of the signal center from the geometrical one. Sometimes, Px(1,0) and Py(0,1) are referred to as monitor k-values. Dominant terms in Eq.(1) are those of Px(i=odd,j=even) and Py(i=even,j=odd), and other terms are small due to the symmetry of the pickup configuration. Fig. 2 shows the setup of the calibration with a coaxial antenna exciting the field in the monitor chamber. Owing to the computer-controlled antenna positioning and data taking, the calibration of one monitor takes only about ten minutes. Fig 3 shows the contour mapping of the monitor coordinates.

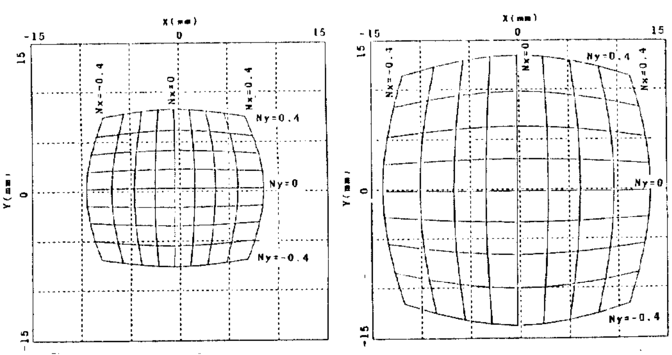

	I/J	0	1	2	3
Px(i,j)	0	-.427	.312	-.108	-.154
	1	19.4	.063	-23.9	---
	2	.095	-.399	---	---
	3	14.8	---	---	---
Py(i,j)	0	-.059	18.1	-.027	7.17
	1	.092	-.010	-.076	---
	2	.010	-10.6	---	---
	3	-.180	---	---	---

(a) racetrack chamber in bending section

	I/J	0	1	2	3
Px(i,j)	0	-.250	.229	-.049	-.660
	1	31.4	.442	-32.9	---
	2	-.096	-.406	---	---
	3	16.0	---	---	---
Py(i,j)	0	-.186	31.7	.425	14.5
	1	.001	.100	-.192	---
	2	.310	-33.2	---	---
	3	-.049	---	---	---

(b) circular chamber in collision section

Fig 3 Contour mapping of position monitors

0018-9499/85/1000-1947$01.00© 1985 IEEE

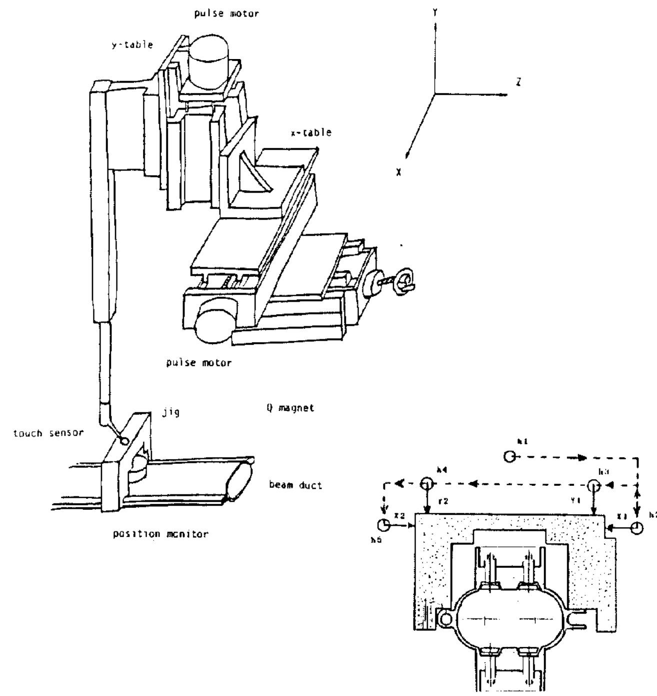

Fig 4 Measuring robot and the course of touch sensor movement

Setting measurement

We measured the geometrical setting of monitor chambers with a measuring robot and a location jig. The robot is set on the standard base on the top of a Q-magnet and the jig, on the other hand, is set on the monitor chamber. The robot arm follows the given course of movement as shown in Fig 4. It starts from the calibrated home positions and moves in a straight line until the head sensor touches the jig. Since the jig has the defined shape and setting to the monitor chamber we know the location of the monitor chamber from the four distance of approach, x's and y's. The accuracy of the geometrical measurement is about 100 microns. The overall beam position accuracy is about 200 microns.

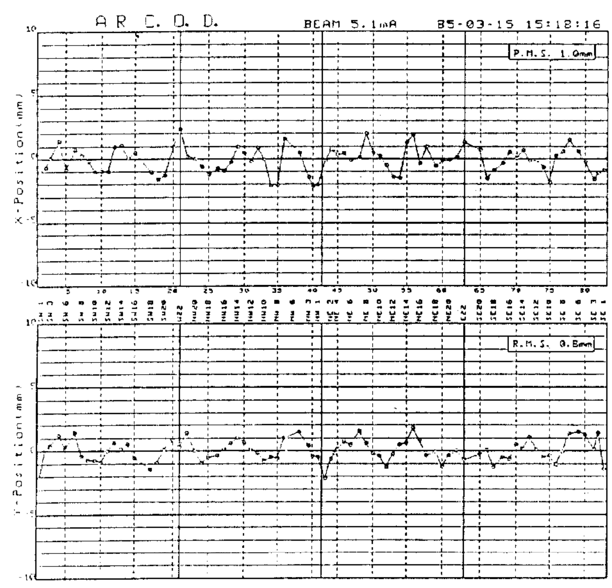

Fig 5 Display of the closed orbit in AR ring

Closed orbit measurement

The measurement of the closed orbit in the four local control proceeds in parallel and takes about 12 seconds. Fig 5 is the display of the orbit on the graphic screen at the control console. We also prepared the display of the voltage output of each monitor electrode as in Fig 6. We consult this display whenever beam orbit looks abnormal because it is very useful to find bad elements in the system.

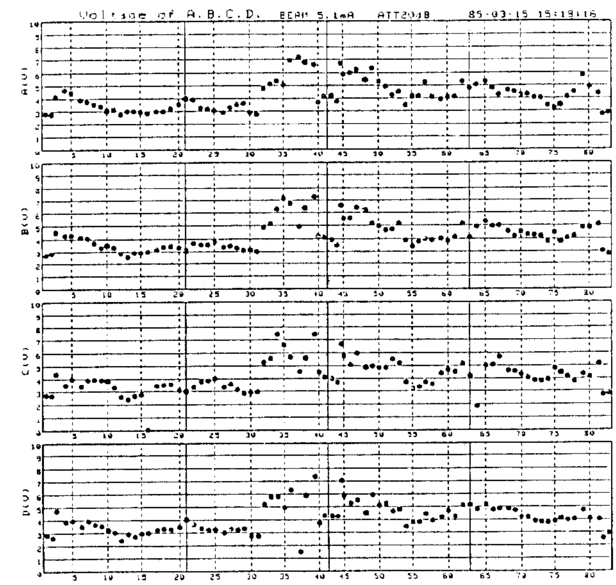

Fig 6 Display of individual electrode outputs

Several studies

Reproducibility

We repeated closed orbit measurements during a beam storage to check the reproducibility of monitors. Figure 7a shows the history of position data of a sample monitor and the beam current in two hours. The statistics of the position data in this measurement is summarized in Table 1. Reproducibility is generally good but five monitors had standard deviation larger than 0.1 mm. It was pushed to a large value, in each case, by a singular position data which appeared once in 110 measurements. We got it when one electrode had a very small output as compared with the other three. It is an abnormal data because one electrode cannot have a small output independently. Such small output was possibly caused by an accidental poor contact at the coaxial switch. We found that we can reduce false data as above by eliminating the data when

$$V_{min} > 0.8 * V2 \quad \text{and} \quad V2 > 0.8 * V_{max} \qquad (2)$$

where $V_{min} \leq V2 \leq V3 \leq V_{max}$ and these are outputs of four electrodes. Actually, Eq (2) is satisfied by the beam within the area of 20 mm x 12 mm in the central region of the chamber. In the later experiment, we met the cases where Eq (2) was not effective because we had plural number of abnormally small output. Hence, we adopted one more criterion; Vmax and Vmin should appear in a diagonal couple of electrodes. This check works well if used together with Eq (2).

Table 1 Distribution of standard deviation in the repeated measurements

	(a) No data check			(b) Check by Eq (2)		
X rms/Y rms	< 0.05	< 0.1	>0.1	< 0.05	< 0.1	>0.1
number of PM	67/63	7/11	5/5	70/67	8/11	1/1

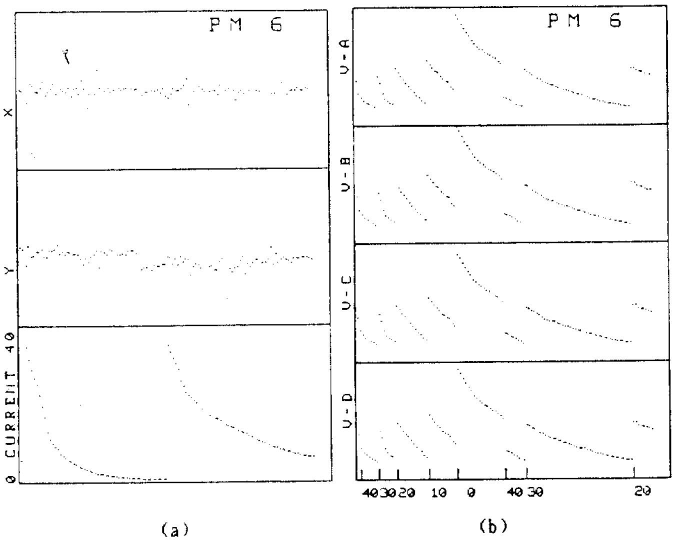

Fig 7 Position monitor data during beam storage

(a) position (0.5 mm range) and beam current (0-40 mA)
(b) electrode outputs (0-10 V)

Beam intensity dependence

Since the beam current decreased from 40 mA to 0.1 mA in the above measurement, Fig 7a shows the performance of electronics at various beam current, too. Fig 7b shows the output voltages of individual electrodes in the same measurements. Step change in the output means the switching of the programmable attenuator. The super-heterodyne circuit has linearity range of about 40 dB and the overall linearity range can be further extended by an external programmable attenuator by 40 dB with 10dB step. However, the full linearity range of the detector circuit is not used because we must adapt the output level to the full range of 11 bit ADC to get enough precision in the normalization. When the programmable attenuator is set at 0 dB, offset of position data is recognized at several monitors. We suspect that this is due to the mismatching at the circuit input and at the pickup electrodes. The effect of mismatching will be largest when four electrodes are unbalanced and there is no attenuation. Therefore, it seems to be adequate to keep the attenuation to some finite level.

Estimation of the setting of unmeasured monitors

Geometrical setting error has not been measured for 20 monitor chambers out of 83 because the measuring robot was not applicable due either to irregular chamber shape or to restriction of space in the tunnel. Hence, reliable position data is not available from these monitors as was demonstrated by the following experiment: orbit correction at the 63 measured monitors was made in two ways, first by using the data of measured monitors only and next by using both measured and unmeasured ones. The first case gave the better result as is shown in Table 2. We proposed a beam experiment in place of the geometrical measurements, to estimate the unmeasured setting errors from the position data of the calibrated monitors. (5)

Table 2 Orbit distortion at measured monitors

correction with	X rms	Y rms	X p-p	Y p-p
measured monitors	0.49	0.19	2.32	0.85
all monitors	0.65	0.27	2.88	1.04

Improvements for MR position monitor

The coefficients Px(1,0) and Py(0,1) which were obtained in the calibration measurement did not fully agree with the analytical calculation in the case of a circular beam duct. In the measurement, the stripped end of the coaxial antenna was set at the position of pickup electrode (position 1 in Fig 8A). The field distribution in this configuration was obtained by "TWA program" (6,7) based on boundary element method (BEM). It showed that the position of the antenna was not adequate because the field is disturbed at the antenna end and, therefore, the pickups did not see such transverse electromagnetic (TEM) field as the beam with light velocity produces. Instead, TEM pattern appears at some distance away from the antenna end (position 2). The measurement agrees with BEM calculation when the antenna position is set so that the pickups see the TEM field. Sensitivity calibration of MR monitors is now proceeding with the improved antenna configuration, but the revised measurement is no longer possible for AR monitors. However, orbit correction of AR is possible even with small error in the sensitivity data because the coordinate origin was correctly obtained in the previous calibration. Therefore, a practical solution will be to replace the coefficients Px(1,0) and Py(0,1) in Eq (1) with the calculated ones.

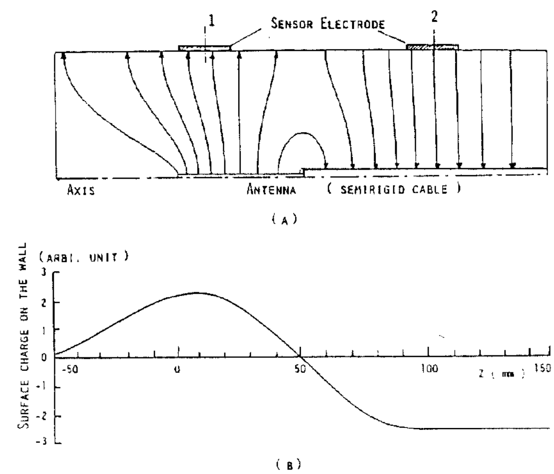

Fig 8 Field distribution in the mapping measurement

References

(1) G. Horikoshi, "Construction and Operation of the TRISTAN Accumulation Ring" in Proc. 5th Symp. Accelerator Science and Technology, Tsukuba, Japan, 1984, pp. 6-8

(2) T. Ieiri, H. Ishii, Y. Mizumachi, A. Ogata, T. Shintake and M. Tejima, "Performance of the Beam Position Monitors of the TRISTAN Accumulation Ring" ibid. pp. 154-156

(3) T. Ieiri, H. Ishii, Y. Mizumachi, A. Ogata, J.-L. Pellegrin and M. Tejima, "Beam Diagnostics of the TRISTAN Accumulation Ring" IEEE Trans. NS-30 (1983) 2356

(4) H. Ishimaru et al., "Construction of Vacuum System for TRISTAN Accumulation Ring" IEEE Trans. NS-30 (1983) 2906

(5) S. Kamada, K. Oide, H. Fukuma, K. Yokoya, K. Nakajima, E. Kikutani and M. Tejima, "Operational results of Optics Handling and Closed Orbit Correction in the TRISTAN Accumulation Ring" contribution to this Conf. (paper L54)

(6) T. Shintake, "Transient Wave Analysis Program using Wave Equation of Vector Potential" contribution to 1984 Linear Accelerator Conf., Darmstadt

(7) T. Shintake, to be published